COMPARATIVE STUDY OF $CaAl_2Fe_{10}O_{19}$ AND $Ca(Co-Sn)Fe_{10}O_{19}$ NANOPARTICLES SYNTHESIZED BY MICROWAVE ASSISTED SOL-GEL COMBUSTION METHOD

GAWALI S.R.[1], MOHARKAR P.R.[2], SABLE S.N.[3], NANOTI V.M.[3] AND REWATKAR K.G.[4]

[1]Department of Physics, Dr. Ambedkar College, Chandrapur, MS, India.
[2]Department of Physics, Arts, Commerce & Science College, Tukum, Chandrapur, MS, India.
[3]Department of Applied Physics, Priyadarshini College of Engineering, Nagpur, MS, India.
[4]Department of Physics, Dr. Ambedkar College, Deeksh Bhuoomi, Nagpur, MS, India.
*Corresponding Author: Email- sanjaygawali500@gmail.com

Abstract- Calcium hexaferrite $CaAl_2Fe_{10}O_{19}$ and $Ca(Co-Sn)Fe_{10}O_{19}$ nanoparticles were synthesized by microwave assisted sol-gel combustion methods. The structural and magnetic properties were characterized by X-ray diffractometer and vibration sample magnetometer, respectively. XRD patterns were refined by Rietveld qualitative method. The XRD data of the both samples have confirmed the formation of single phase M-type hexagonal ferrites. The space group for the samples is observed to be P_{63}/mmc. The simultaneous or coupled divalent and tetravalent substitution of Co^{2+} and Sn^{4+} for Fe^{3+} ions in calcium hexaferrite greatly helps to improvise the magnetic parameters such as coercivity, remanent magnetization, saturation magnetization, etc than trivalent substitution of Al^{3+} for Fe^{3+} ion in calcium hexaferrite. The coupled divalent and tetravalent substitution in calcium ferrite reduces the particle size from 93.97 nm to 11 nm than trivalent substitution in calcium hexaferrite .
Keywords- Hexaferrites, Nanoparticles, Magnetic parameters, Microwave Induced Sol-Gel Combustion Route, Coercivity, Remenance.

Introduction

The M-type calcium hexaferrite, due to its excellent chemical stability, good thermal durability, corrosion resistivity, unique electrical and magnetic properties, has extensive applications in recording devices [1], telecommunication [2], magnetooptical and microwave devices [3]. This material covers a wide field of technological applications, from microwave to radio frequencies, due to its high electrical resistivity [4]. The properties of the ferrites are strongly influenced by their composition and synthesis method [5]. The M-type calcium ferrite crystallizes in an hexagonal structure with 64 ions per unit cell on 11 different symmetry sites. The 24 Fe3+ atoms are distributed over five distinct sites: three octahedral sites (12k, 2a and $4f_2$), one tetrahedral (4f1) site and one bipyramidal site (2b). The magnetic structure given by the Gorter model is ferromagnetic with five different sublattices, three parallel (12k, 2a and 2b) and two antiparallel ($4f_1$ and $4f_2$) which are coupled by super exchange interactions through the O^{2-} ions.

The intrinsic magnetic properties of M-type ferrites can be improved by partial substitution of Ba or Fe, or both [6]. For example, it has recently been shown that La-Co substituted $SrFe_{12}O_{19}$ferrites have improved magnetic properties [7].

In this paper, a series of $CaAl_2Fe_{10}O_{19}$ and $Ca(Co-Sn)Fe_{10}O_{19}$ nanoparticles samples were synthesized by sol-gel combustion method and the comparative study of structural, morphological and magnetic properties of synthesized samples have been reported.

Experimental procedure

The Al and Co-Sn ions substituted calcium ferrites were synthesized by microwave assisted sol-gel combustion method. The AR

grade calcium nitrate $Ca(NO_3)_2 \cdot 4H_2O$, iron nitrate $Fe(NO_3)_3 \cdot 9H_2O$, aluminum nitrate $Al(NO_3)_3 \cdot 9H_2O$, $Co(NO3)_2 \cdot 6H2O$, $SnCl4$ and urea $CO(NH_2)_2$ (analytical reagent grade) were used as raw components. Stoichiometric amount of metal nitrates / metal chloride was dissolved completely in deionized water. The urea $CO(NH_2)_2$ was also dissolved in deionized water. The solutions as prepared were mixed together to form a homogeneous transparent aqueous solution. The aqueous solution was then heated into the microwave oven. After few minutes aqueous solution get converted into wet gel by evaporating the water. After the wet gel reaches the point of spontaneous combustion, it begins burning and becomes a solid which burns at a temperature above 1000 °C. The combustion is not completed until all the flammable substances are consumed and the resulting material is a loose, highly friable substance exhibiting voids and pores formed by escaping gases during combustion reaction. The ash Al and Co-Sn substituted calcium ferrite were obtained. These samples were finally annealed at 950 °C for 2 h at a heating rate of 5 °C/min.

Characterization

The phases of the synthesized ferrites powder was identified at room temperature using X-ray diffractometer (Philips Holland XRD System Model No. PW 1710, CuKα, λ=1.5405 Å).

The values of lattice constants 'a' and 'c', X-ray density (ρ_{x-ray}), bulk density (ρ_m), porosity (P) and the unit cell volumes (V_{cell}) were calculated by following equations and are tabulated in Table 1.

$$\frac{1}{d^2} = \frac{4(h^2 + k^2 + hk)}{3a^2} + \frac{l^2}{c^2} \tag{1}$$

$$\rho_{x-ray} = \frac{2M}{N_A V_{cell}} \tag{2}$$

$$\rho_m = \frac{m}{\pi r^2 h} \tag{3}$$

$$P = 1 - \frac{\rho_m}{\rho_{x-ray}} \tag{4}$$

$$V_{cell} = 0.8666a^2 \tag{5}$$

where a and c are lattice constants, M is the molar mass, m the mass of pellets, r radius of the pellets, N_A Avogadro's number and V_{cell} the unit cell volume.

The morphological features of the samples were examined by transmission electron microscopy (TEM Philips Model No. CM 200). The magnetic property of the substituted ferrite was measured with vibrating sample magnetometer (VSM Lakeshore Model No. 665).

Results

The X-ray diffraction spectra of the powders of Al and Co-Sn ions substituted calcium ferrites are shown in Fig. 1. The XRD data are analyzed by using computer software PCPDF Win, PowderX and FullProf Suite. By comparing the patterns with JCPDS, the phases in the different samples are determined. It was observed that all peaks were perfectly matched with standard pattern, confirming the single magnetoplumbite phase in the reported samples. The space group for the samples is observed to be SG: P6₃/mmc (No. 194). XRD pattern also show few noisy peaks which may be due to two reasons, firstly, the crystallite size are very small, secondly, it may be due to instrumental error.
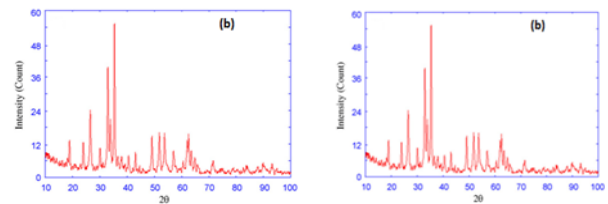

Fig. 1- (a) Sample CaAl₂Fe₁₀O₁₉ and (b) Sample Ca(Co-Sn) Fe₁₀O₁₉: X-ray diffraction spectra

The Lattice constants 'a' and 'c', X-ray densities 'ρ_{x-ray}', bulk densities 'ρ_m' and porosity of Al and Co-Sn ions substituted calcium ferrite samples at room temperature are enumerated in the Table1. The bulk density of the substituted samples is lower than the X-ray density which indicates the presence of pores in the synthesized samples

Fig 2 shows TEM micrograph of Al and couped Co-Sn substituted calcium ferrite. It is observed from TEM micrograph that the average particle size of Al and coupled Co-Sn substituted calcium ferrite are 120, 93.97 and 11 nm. The average particle size of Co-Sn substituted calcium ferrite is lower than that of Al³⁺ ion substituted calcium. These sizes are small enough for obtaining the suitable signals-to-noise ratio in the high density recording media. It is reasonable to confirm that the particle size of coupled divalent Co^{2+} and tetravalent Sn^{4+} ions does remain more responsive to particle size of substituted calcium ferrite than that for trivalent Al^{3+} ion substitution in calcium ferrite [8].
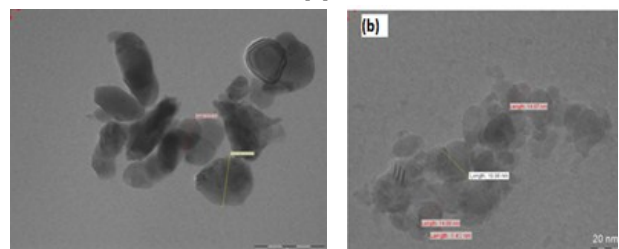

Fig. 2- (a) Sample CaAl₂Fe₁₀O₁₉ and (b) Sample Ca(Co-Sn) Fe₁₀O₁₉: TEM micrograph

VSM

The magnetic hysteresis loop measurements of the Al and coupled Co-Sn substituted calcium ferrites is shown in Fig. 3. The values of the magnetic parameters of these compounds obtained from the data of Fig. 2 are tabulated in Table 2. In Table 2 we found that the values of saturation magnetization M_s and remanent magnetization M_r and coercivity H_c increase with substituent. In the magnetic structure of $CaFe_{12}O_{19}$, the Fe^{3+} ions were arranged in five different kind of spin sublattices, 12k, 4f₁, 4f₂, 2a and 2b. The magnetic moment of Fe^{3+} ions were parallel with hexagonal c-axis at six octahedral coordination of spin sublattices (12k), one octahedral coordination of spin sublattice (2a) and one hexahedral coordination of spin sublattice (2b). Other than these three sublattices, the magnetic moments of other four Fe^{3+} ions were antiparallel with the hexagonal c-axis at two octahedral coordination of spin sublattices (4f₂) and two tetrahedral coordination of spin sublattices (4f₁). In the Co-Sn ions substituted calcium hexaferrite, Fe^{3+} ions are partially replaced by the equal amount of Co^{2+} and Sn^{4+} ions. Co^{2+} ions prefer to replace the spin down of Fe^{3+} ions in

tetrahedral sublattices $(4f_1)$ and Sn^{4+} ions substitute either for spin up or spin down of Fe^{3+} ion in octahedral sublattices [9-10]. Introduction of Co^{2+} ions into the tetrahedral sites would not change the net magnetization of materials, but the replacement of Sn^{4+} ions into octahedral sites caused the variation of the net magnetization of the materials. In case of aluminium ion substituted calcium ferrite, Fe^{3+} ions of spin down in tetrahedral sublattice $(4f_1)$ are replaced by non-magnetic Al^{3+} ions, thereby net magnetization of the Al^{3+} ion substituted material which is very low as compared with that of Co-Sn substituted material. Thus the divalent and tetravalent substitution of Co-Sn in calcium ferrite enhances the magnetic properties than that of trivalent substitution of aluminium into calcium ferrite.

The usefulness of a particular magnetic material for a specific application depends on its relevant properties. One of these properties is the coercivity of the M-type hexaferrites. High coercivity is the demand of a hard magnet while low coercivity is the need of a soft magnet. The former is needed for energy storage applications. The later is needed for information storage recording media [11]. The origin of coercivity lies in the magnetic anisotropy, which is particularly uniaxial for the hexagonal close packing of the hexaferrites. In view of improvisation of the hexaferrites, testing various magnetic properties is of great importance. The coercivity and remanence of the synthesized samples are found to be in the range where they could be used in the applications mentioned earlier as tabulated in Table 2.

The coercivity (H_c) increases with the Co-Sn substitutent into calcium ferrite than that with aluminium substituent into calcium ferrite. The observed increase in coercivity is because of the increase in magnetocrystalline anisotropy. These results are in agreement with many researcher's results [12-14]. Furthermore, the increase in coercivity of Co-Sn substituted calcium hexaferrite is due to finer grains [15].
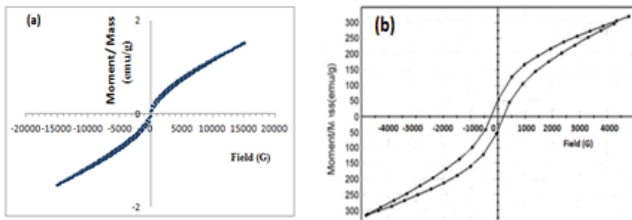

Fig. 3- B-H curve-(a) Sample $CaAl_2Fe_{10}O_{19}$ and (b) sample $Ca(Co-Sn)Fe_{10}O_{19}$: Hysteresis loops of samples

Table 2- The magnetic properties of substituted calcium hexaferrite

Sample	M_s (emu/g)	M_r (emu/g)	H_c (Oe)
$CaAl_2Fe_{10}O_{19}$	1.51	0.18	21.13
$Ca(Co-Sn)Fe_{10}O_{19}$	328.79	63.21	479

Conclusions

The samples of aluminium and coupled Co-Sn substituted calcium hexaferrites were synthesized by microwave assisted sol-gel combustion method. The XRD analysis confirm the formation of single phase M-type hexagonal ferrite. The space group synthesized samples is found to be $P6_3/mmc$. From TEM of the sample, the average particle size is found to be in the nano-range ($\approx 11nm$). The reduction of particle size of hexaferrites samples to nanorange greatly improves the magnetic properties such as saturation magnetization, remanent magnetization and coercivity. Thus, the coupled Co-Sn substituted calcium hexaferrite have superior magnetic properties than that of aluminium substituted calcium hexaferrite.

References

[1] Palla B.J., Shah D.O., Casillas P.G., Aquino J.M. (1999) *J. Nanopart Res*. 1, 215.
[2] Costa A.C.F.M., Tortella E., Morelli M.R., Kininami R.H.G.A. (2003) *J. Magn. Magn. Mater*. 256, 174.
[3] Qiu J., Gu M., Shen H. (2005) *J. Magn. Magn. Mater*. 295, 263.
[4] Peng C.H., Hwang C.C., Wan J., Tsai J.S., Chen S.Y. (2005) *Mater. Sci. Eng. B* 117, 27.
[5] U. Ghazanfar, S.A. Siddiqi, G. Abbas, Mater. Sci. Eng. B 118 (2005) 132.
[6] Robinson T.M. (1990) *J. Mater. Res. Bull*., 25, 1401.
[7] Mocuta H., Lechevallier L., Le J.M., Breton J.M. (2004) *J., Alloys and Comp*., 364, 48.
[8] Sable S.N., Rewatkar K.G., Nanoti V.M. (2010) *J. Mater. Sci. Eng. B*. 168, 156-160.
[9] Mali A., Ataie A. (2005) *Journal of Alloys and Compounds* 399, 245-250.
[10] Ounnunkad S., Winotai P. (2006) *Journal of Magnetism and Magnetic Materials* 301, 292-300.
[11] Rezlescu N., Doroftei C., Rezlescu E., Popa P.D. (2008) *Journal of Alloys and Compounds* 451, 492-496.
[12] Tenaud P., Morel A., Cool F., Le Breton J.M., Lechevallier L. (2004) *J. Alloys Compd*. 370, 331.
[13] Le Breton J.M., Wiesinger G., Tellez Blanco C., Isnard O., Teillet J., Grössinger R., Morel A., Cools F., Tenaud P. (2000) *Int. Conf. on Ferrites, Kyoto, Japan*, 18-21, 199.
[14] van Dipen A.M., Lotgering F.K. (1974) *J. Phys. Chem. Solids* 35, 1641.
[15] Ounnunkad S. and Winotai P. (2006) *J. Magn. Magn. Mater*. 301, 292-300.

Table 1- Lattice constants 'a' and 'c', X-ray densities 'px-ray', bulk densities 'pm', porosity 'P' and particle size (D) of Al and Co-Sn substituted calcium ferrite samples at room temperature

Sample	a (Å)	c (Å)	ρ_{x-ray} (g cm^{-3})	ρ_m (g cm^{-3})	P (%)	D (nm)
$CaAl_2Fe_{10}O_{19}$	5.8179	22.1353	4.907	2.685	45.28	93.97
$Ca(Co-Sn)Fe_{10}O_{19}$	5.8436	21.5166				11